

³N. D'Angelo and R. W. Motley, Phys. Fluids 6, 422 (1963).

⁴H. Lashinsky, Phys. Rev. Letters 12, 121 (1964).

⁵N. Kroll and M. Rosenbluth, Phys. Fluids 6, 254 (1963); L. I. Rudakov and R. Z. Sagdeev, Suppl. Nucl. Fusion, Pt. 2, 823 (1962).

⁶V. P. Silin, Zh. Eksperim. i Teor. Fiz. 44, 1271

(1963) [translation: Soviet Phys.-JETP 17, 857 (1963)].

⁷K. V. Roberts and J. B. Taylor, Phys. Rev. Letters 8, 197 (1962).

⁸A. Y. Wong, N. D'Angelo, and R. W. Motley, Phys. Rev. Letters 9, 415 (1962).

⁹A. A. Galeev, S. S. Moiseev, and R. Z. Sagdeev, At. Energ. 15, 451 (1963).

ABSOLUTE INSTABILITIES WITH DRIFTED HELICONS

Abraham Bers

Department of Electrical Engineering and Research Laboratory of Electronics,*
Massachusetts Institute of Technology, Cambridge, Massachusetts

and

A. L. McWhorter

Department of Electrical Engineering and Lincoln Laboratory,†
Massachusetts Institute of Technology, Cambridge, Massachusetts

(Received 6 August 1965)

In this Letter we report analytic results based on an exact computer analysis of helicon-wave instabilities in a drifted electron-hole plasma. Previous analyses¹⁻³ have not distinguished between absolute (nonconvective) instabilities, which correspond to growth in time at every point in space or an oscillator, and convective instabilities, which correspond to spatial amplification over a range of real frequencies. It has been tacitly assumed that in order to have spatial amplification, it is sufficient for the dispersion relation to yield complex k 's for some real ω provided that complex ω 's also exist for some real k 's; whereas, in fact, one must in addition show that no absolute instabilities exist, for otherwise oscillations will occur at the frequency and wave number of the absolute instability. In view of the considerable experimental work⁴⁻⁷ in this area, it would seem most important to clarify the theoretical picture. Our results, which are based on a recently developed technique for determining the nature of instabilities,⁸ show for example that in InSb with equal electron and hole concentrations, an absolute instability should appear above a threshold magnetic field, at an arbitrarily small electric field. Furthermore, from our results we develop a physical picture of the instabilities, radically different from the one given by either Bok and Nozières¹ or Misawa,² and show it to be correct in that it predicts the exact computer results. This pic-

ture has the same basis as the one recently and independently described by Hasegawa,³ who failed, however, to correctly identify the nature of the instability.

We restrict our discussion here to isotropic and nondegenerate semiconductors, and use a hydrodynamic description⁹ of the free carriers. The dispersion relation for transverse waves, $\exp(i\omega t - ikz)$, with k along the applied magnetic field B_0 , and electrons and holes counterstreaming parallel to B_0 with velocities v_e and v_h , respectively, is¹⁰

$$\omega^2 - c^2 k^2 = \frac{\omega_{pe}^2 (\omega - kv_e)}{(\omega - kv_e - i\nu_e \pm \omega_{ce})} + \frac{\omega_{ph}^2 (\omega + kv_h)}{(\omega + kv_h - i\nu_h \mp \omega_{ch})}, \quad (1)$$

where c is the velocity of light, ω_{pe} and ω_{ph} the electron and hole plasma frequencies, ω_{ce} and ω_{ch} the electron and hole cyclotron frequencies, and ν_e and ν_h the electron and hole collision frequencies. The stability analysis consists in first mapping from (1) the real k axis into the complex ω plane; if part of the real k axis maps into the lower half ω plane the system may exhibit some kind of instability. Any portion of the lower half of the ω plane containing a mapping of part of the real k axis is then investigated by mapping lines of constant $\text{Re}\omega$

with increasing $\text{Im}\omega$ into the complex k plane. In general there will be several roots for k as a function of ω and hence several contours in the k plane for each line of constant $\text{Re}\omega$ in the ω plane. If for any $\text{Re}\omega$ two contours corresponding to different roots start for large negative $\text{Im}\omega$ from opposite sides of the real k axis and meet for some $\text{Im}\omega < 0$, we have an absolute instability; the location of the branch point in the lower half of the ω plane corresponding to the meeting point (saddle point) in the k plane gives the frequency and temporal growth rate of the absolute instability. If no saddle point of this type occurs, but if a contour of constant $\text{Re}\omega$ crosses the real k axis, we have a convective instability; the value of $\text{Im}k$ at $\text{Im}\omega = 0$ gives the spatial growth rate at the frequency being examined. Such an analysis of the dispersion relation (1) was carried out with the aid of the M.I.T. Electronics System Laboratory computer display console and Project MAC.¹¹ Figure 1 shows an example of k -plane contours (of the lower half ω plane) for InSb in a variable applied magnetic field and electric field sufficient to produce avalanche. We note that below 1400 G the instability is con-

vective, at about 1400 G an absolute instability sets in at a complex value of k , and as the magnetic field is raised the absolute instability remains. We have analyzed (1) for a great variety of physical parameters. Here we would like to present the physical picture of the instabilities that has emerged from these exact computations and to summarize the major results of importance to current experiments in semiconductor plasmas.⁴⁻⁷

In the case of a plasma with $\omega_{ce}/\nu_e > 1$ and $\omega_{ch}/\nu_h < 1$, as is the case for InSb with moderate magnetic fields, the drifting electrons provide a negative-energy wave¹² (Fig. 2) with both forward and backward group velocities; the holes act as a resistive medium background. As is well known, negative-energy waves in the presence of a resistive background become unstable. The usual resistive medium instability¹³ is with a forward group velocity, negative-energy wave, and is therefore convective. The new feature with drifted helicons is that the negative-energy wave can have zero group velocity, and hence the instability can be absolute.¹⁴ Indeed, exact calculations show that the onset of the absolute instability is at the

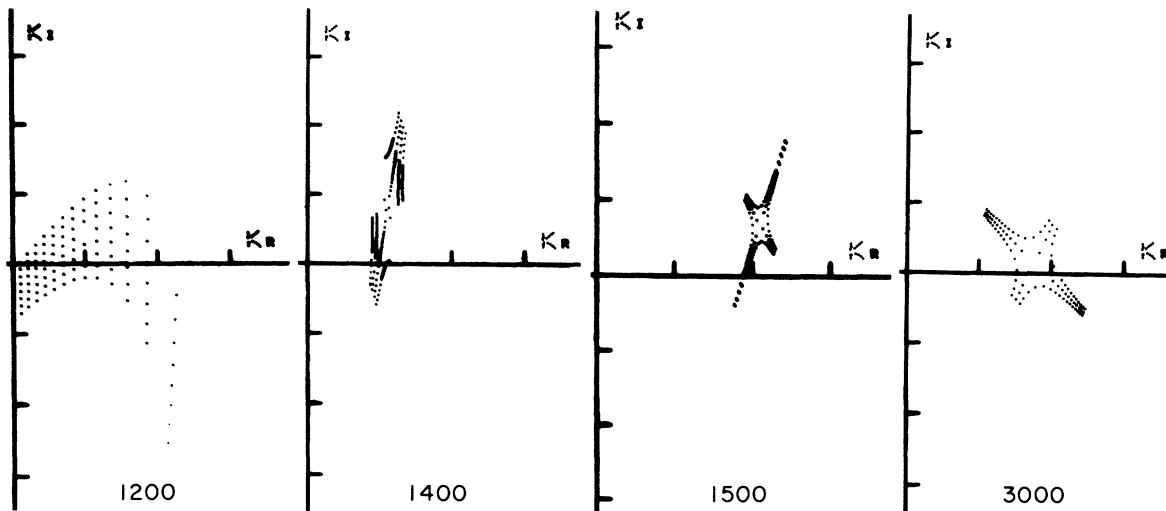


FIG. 1. Computer display of the mapping of the lower half ω plane into the complex k plane using the dispersion relation of Eq. (1), for an electric field of 200 V/cm and several values of applied magnetic field. Assumed parameter values, appropriate for InSb at 77°K under avalanche conditions: $m_e^* = 0.013m_0$; $m_h^* = 0.18m_0$; $\mu_e = 5 \times 10^5$ cm²/V Sec; $\mu_h = 10^4$ cm²/V sec; $n_e = n_h = 10^{16}$ /cm³. In the k -plane display for 1200 G only the root that crosses the real k axis is shown. The straight lines of dots, essentially parallel to the imaginary k axis, have $\text{Re}\omega$ constant; they start in the lower half k plane for large $\text{Im}\omega < 0$ and end at $\text{Im}\omega = 0$. The value of $\text{Im}k$ at $\text{Im}\omega = 0$ gives the spatial growth rate at the corresponding $\text{Re}\omega$. In all other displays only the two roots that indicate the absolute instability are shown. For large $\text{Im}\omega$ one root is above the real k axis and the other is below. For constant $\text{Re}\omega$ the two roots approach each other as $\text{Im}\omega$ increases, one of them crosses the real k axis, and as $\text{Im}\omega$ goes to zero the roots separate again. As $\text{Re}\omega$ is increased the two roots interchange their direction of separation as $\text{Im}\omega$ goes to zero, giving a saddle map. This indicates that for some $\text{Re}\omega$ the roots will meet at some $\text{Im}\omega < 0$; the location of this branch point of $k(\omega)$ gives the frequency and temporal growth rate of the absolute instability.

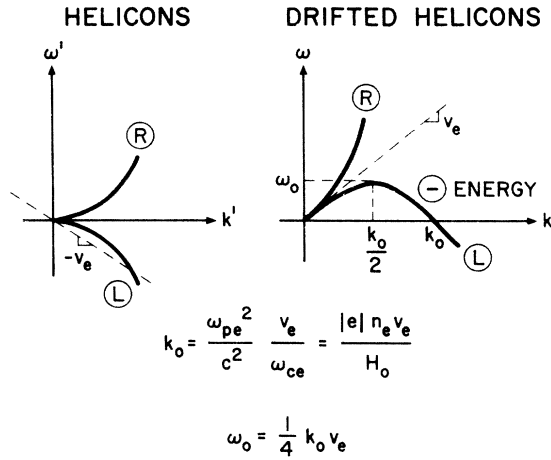


FIG. 2. Dispersion diagrams for helicons and drifted helicons; R stands for right polarized and L for left polarized. The (ω, k) plot is obtained from the (ω', k') plot through the transformation law for waves in two coordinate systems moving with relative velocity v_e , the electron drift velocity; the part of the L wave that changes its sign in frequency becomes a negative-energy wave. It is assumed that $(\omega_{pe}/\omega_{ce})^2(v_e/c)^2 \ll 1$.

frequency ω_0 and wave number $k_0/2$, given in Fig. 2, where the negative-energy wave branch of the drifted helicons has zero group velocity. As ω_{ce}/v_e is decreased, the backward wave becomes damped, and the instability changes to a convective one, in the direction of v_e , and extends for frequencies from zero to about ω_0 (see, e.g., Fig. 1 at 1200 G). The condition for the onset of the absolute instability can be obtained from (1) by requiring that the appropriate branch point of $k(\omega)$ just cross into the lower half ω plane. For $\omega_{ch}/v_h \ll 1$, $kv_e \ll \omega_{ce}$, $kv_h \ll \omega_{ch}$, and $k \gg \omega/c$, we obtain that

$$(v_e/\omega_{ce})^2 \omega_{pe}^2/v_e < \omega_{ph}^2/v_h \quad (2)$$

is required for the instability to change from convective to absolute. The growth rate in time of the absolute instability is given by the imaginary part of the branch point in the ω plane,

$$\omega_{si} = \frac{(\omega_{pe}^2/\omega_{ce}^2)[(\omega_{pe}^2/\omega_{ce}^2)v_e - \omega_{ph}^2/v_h]}{\omega_0(\omega_{pe}^4/\omega_{ce}^2) + [(\omega_{pe}^2/\omega_{ce}^2)v_e + \omega_{ph}^2/v_h]^2}, \quad (3)$$

where ω_0 is as given in Fig. 2. These also are borne out by the exact computations. Finally, as is clear from the transformations of ω and k in Fig. 2, the one-dimensional treatment

predicts that the negative-energy branch will exist for arbitrarily small drift velocities. Hence, if condition (2) is satisfied, the absolute instability will also occur for arbitrarily small drifts (i.e., small applied electric fields), albeit at correspondingly lower frequencies and with lower growth rates. In practice, since lowering v_e decreases k_0 (see Fig. 2), the lowest drift velocity for which these considerations apply will be limited by boundary effects.

In conclusion, we point out that the one-dimensional theory for drifted helicons, with $\omega_{ce}/v_e > 1$ and $\omega_{ch}/v_h \ll 1$ (e.g., in InSb at moderate magnetic fields), predicts that an absolute instability will exist when inequality (2) is satisfied. The physical picture is that the electron negative-energy wave with both positive and negative group velocities becomes unstable (in time at every point in space) in the presence of the resistive medium background provided by the holes. The absolute instability will occur at a definite frequency ω_0 (Fig. 2), and the system will build up as an oscillator with an initial time growth rate given by Eq. (3). The amplifier solutions (complex k 's for real ω) of Eq. (1) are then meaningless. We have shown these considerations to be correct in that they predict the exact computer stability analysis of Eq. (1).

We would like to acknowledge the assistance of Mr. Wei Y. Chang in carrying out some of the programming and computations.

*This work was supported in part by the Joint Services Electronics Program under Contract No. DA36-039-AMC-03200(E), and by the National Science Foundation (Grant No. GK-57).

†Operated with support from the U. S. Air Force.

¹J. Bok and P. Nozières, *J. Phys. Chem. Solids* **24**, 709 (1963).

²T. Misawa, *J. Appl. Phys. (Japan)* **2**, 500 (1963).

³A. Hasegawa, *J. Phys. Soc. Japan* **20**, 1072 (1965).

⁴R. D. Larrabee and W. A. Hicinbotham, Jr., in *Plasma Effects in Solids* (Dunod, Paris, 1965), p. 181; M. C. Steele, *ibid.*, p. 189.

⁵S. J. Buchsbaum, A. G. Chynoweth, and W. L. Feldman, *Appl. Phys. Letters* **6**, 67 (1965).

⁶C. Nanney, *Bull. Am. Phys. Soc.* **9**, 648 (1964).

⁷D. J. Bartelink, *Phys. Rev. Letters* **12**, 479 (1964); *Bull. Am. Phys. Soc.* **10**, 384 (1965).

⁸A. Bers and R. J. Briggs, M.I.T. Research Laboratory of Electronics Quarterly Progress Report No. 71, 15 October 1963 (unpublished), pp. 122-131; *Bull. Am. Phys. Soc.* **9**, 304 (1964). R. J. Briggs, *Electron Stream Interaction with Plasmas* (M.I.T. Press, Cambridge, Massachusetts, 1964).

⁹For ω and k in the helicon regime of interest here, Doppler-shifted cyclotron resonance effects are negligible.

¹⁰This dispersion relation is the same as that used in references 1-3. It should be noted that the self-magnetic field of the dc current has not been included. It may not be possible to neglect this field compared to the applied magnetic field without simultaneously endangering the one-dimensional assumption. This requires further study.

¹¹A. Bers and J. D. Mills, M.I.T. Research Laboratory of Electronics and Project MAC Report (to be published).

lished).

¹²R. J. Briggs and A. Bers, M.I.T. Research Laboratory of Electronics Quarterly Progress Report No. 67, 15 October 1962 (unpublished), pp. 35-43.

¹³C. K. Birdsall, G. R. Brewer, and A. V. Haeff, Proc. IRE 41, 865 (1953).

¹⁴In the absence of collisions, and for gaseous plasmas, an absolute instability in this regime was pointed out by R. J. Briggs and A. Bers, in Proceedings of the Fourth Symposium on Engineering Aspects of Magneto-hydrodynamics, University of California, Berkeley, California, April 1963 (unpublished), pp. 23-30.

CHARGE DISTRIBUTIONS OF Ca⁴⁰ AND Ca⁴⁴ FROM 250-MeV ELECTRON SCATTERING*†

R. Hofstadter,‡ G. K. Nöldeke,§ K. J. van Oostrum,|| L. R. Suelzle, and M. R. Yearian
High-Energy Physics Laboratory and Department of Physics, Stanford University, Stanford, California

and

B. C. Clark and R. Herman

Research Laboratories, General Motors Corporation, Warren, Michigan

and

D. G. Ravenhall

University of Illinois, Urbana, Illinois
(Received 18 October 1965)

In this paper we report new information on differences between the charge distributions of Ca⁴⁰ and of Ca⁴⁴, obtained by means of elastic scattering of 250-MeV electrons.¹ As is the case with single isotopes, more detail can be detected with this method than with muonic or optical isotope shifts. An interesting result was obtained recently, by the muonic-atom method, that the equivalent radius $R = [5\langle r^2 \rangle / 3]^{1/2}$ increases by only about 0.8%, compared with the $A^{1/3}$ prediction of 3.2%.^{2,3} We agree with this result and find additionally that this 0.8% increase of R arises from a 2.2% increase in the half-radius of the charge distribution, together with a 1.6% decrease in the skin thickness.

We recall that the $A^{1/3}$ dependence of the nuclear half-radius, c , deduced from electron scattering, came from experiments on seven nuclei, Ca to Bi, widely spread through the periodic table.⁴ It is thus measured only as a gross property for large variations in A . Either for simplicity, or to utilize the fact that an $A^{1/3}$ variation of c with A , coupled with a constant surface thickness, produces a central nucleon density roughly independent of A , the

detailed $A^{1/3}$ dependence of c has perhaps acquired a more solid status than present experiment warrants.^{5,6} What the muonic x-ray measurements obtained, and what our new electron scattering results probe in greater detail, is the modulation, possibly due to nuclear shell structure, of the gross $A^{1/3}$ dependence of the nuclear size.

The basic idea, suggested some time ago,⁷ is to measure experimentally and analyze theoretically not the differential cross sections of the separate isotopes, but the isotopic difference in these quantities or, equivalently, the ratio of the cross sections. Most of the systematic experimental errors associated with an absolute cross-section measurement are eliminated by taking the ratio of the cross sections. Theoretically, the connection with the isotopic ratio of charge densities is also made more directly.

We have carried out this comparative experiment on Ca⁴⁰ and Ca⁴⁴ by alternating the targets and measuring the cross sections for both isotopes under the same experimental conditions. The basic method has been described previously.⁸ An improvement in technique has